First Insights into Electrografted Polymers by AFM-Based Force Spectroscopy

Stéphane Cuenot,[⊥,†] Sabine Gabriel,[‡] Robert Jérôme,[‡] Christine Jérôme,*[,‡] Charles-André Fustin,[§] Alain M. Jonas,[†] and Anne-Sophie Duwez*[,†,#]

Unité POLY and CeRMiN, Université catholique de Louvain, Place Croix du Sud 1, B-1348 Louvain-la-Neuve, Belgium; CERM, Université de Liège, B6 Sart-Tilman, B-4000 Liège, Belgium; and Unité CMAT and CeRMiN, Université catholique de Louvain, Place L. Pasteur 1, B-1348 Louvain-la-Neuve, Belgium

Received April 12, 2006; Revised Manuscript Received July 4, 2006

ABSTRACT: The very first characterization of the structural properties of polymer films obtained by electrografting is reported. AFM-based force spectroscopy was used to investigate poly-*N*-succinimidyl acrylate (PNSA) layers electrografted directly from a silicon substrate. Quantitative analysis of compression profiles obtained in a good solvent and single molecule bridging interaction, in light of the Alexander−de Gennes model, gave access to the grafting density and degree of polymerization. A high swelling capacity has been evidenced. This report is the first evidence that polymers obtained by cathodic electrografting are in fact brush systems, and consequently the first evidence that a polymer brush can be obtained from a direct "grafting from" method, without any intermediate layer.

Introduction

Silicon plays a key role in the development of micro- and optoelectronic devices, microelectromechanical machines, and chemo- or bio(nano)sensors. The design of the chemical, physical, and mechanical properties of such silicon-based devices requires their surface functionalization.[1−3] Grafted polymer brushes have been proved to be an ideal choice in sensor applications for several reasons. They are chemically tethered to the surface at one end, and this is crucial for having a sufficient long-term stability of the films in different environments. This is a significant advantage over spin-coated films. Virtually any chemistry can be designed into the layer thanks to the large variety of suitable monomers. The mechanical flexibility can be tailored by changing the polymer chain density. Their specific sensing properties, like their high sensitivity to solvent vapors, enable their use as sensors for trace gas detection.[4] Their ability to swell or collapse as a function of solvent quality can be exploited in encapsulation-release applications. These unique qualities gave rise to intense theoretical and experimental development of polymer brush systems and particularly "grafting from" methods.[5−8] Numerous grafting strategies have been proposed, based on multistep procedures, sometimes complex, requiring the use of specific coupling chemistry to attach initiators on surfaces.

Electrografting is a very simple one-step procedure to fabricate polymer films tightly attached to their substrate. The substrate is simply dipped into the monomer solution and is polarized in the cathodic range using a classical three-electrode setup. It is an electroinitiated process that requires a charged electrode only for the grafting step.[9] The chain propagation that follows is a chemical process that does not need current for being sustained. The polyaddition is stopped by noncontrolled termination reactions, which limit the film thickness. An increase of the monomer concentration in the electrochemical bath leads to an increase of the film thickness, as reported by Baute et al.,[9a] the chain propagation being faster when the monomer concentration is increased. Electrografting has contributed to substantial evolution in applications such as protective coatings against corrosion,[10] as antibacterial coatings,[11] as a primer for the immobilization of biomolecules,[12,13] surface modification of biomedical devices such as stents,[14] and the preparation of protein-repellent surfaces.[15] The organic films obtained by electrografting have been characterized macroscopically in air,[9] but so far nothing is known about their structural properties.

Scheme 1. Electrografting Process of *N*-Succinimidyl Acrylate (NSA)

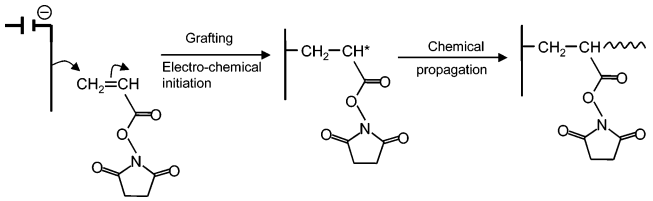

Here we investigate electrografted films in solution by AFM-based force spectroscopy.[16] The polymer selected for grafting is poly-*N*-succinimidyl acrylate (PNSA), and two different concentrations (0.1 and 1 M) of the monomer have been investigated. Silicon substrates were dipped into the NSA solution and were polarized in the cathodic range using a classical three-electrode setup as described in the Experimental Section. The electrografting process is schematized in Scheme 1. The reason for choosing NSA as monomer is based on its high room temperature reactivity toward nucleophiles, paving the way to further easy derivatization, e.g., by reaction with amino derivatives such as biomacromolecules, opening the possibility to use the polymer film as an anchoring layer for biodevices.[13]

Results and Discussion

Grafting Density. Figure 1a shows the approach profile obtained in *N*,*N*-dimethylformamide (DMF, a good solvent for

[†] Unité POLY and CeRMiN, Université catholique de Louvain.
[‡] Université de Liège.
[§] Unité CMAT and CeRMiN, Université catholique de Louvain.
[⊥] Present address: Institut des Matériaux Jean Rouxel, Rue de la Houssinière 2, F-44322 Nantes cedex 3, France.
[#] Present address: Department of Chemistry, University of Liège, B6a Sart-Tilman, B-4000 Liège, Belgium.
* To whom correspondence should be addressed. E-mail: asduwez@ulg.ac.be or c.jerome@ulg.ac.be.

10.1021/ma060824m CCC: $33.50
Published on Web 10/26/2006

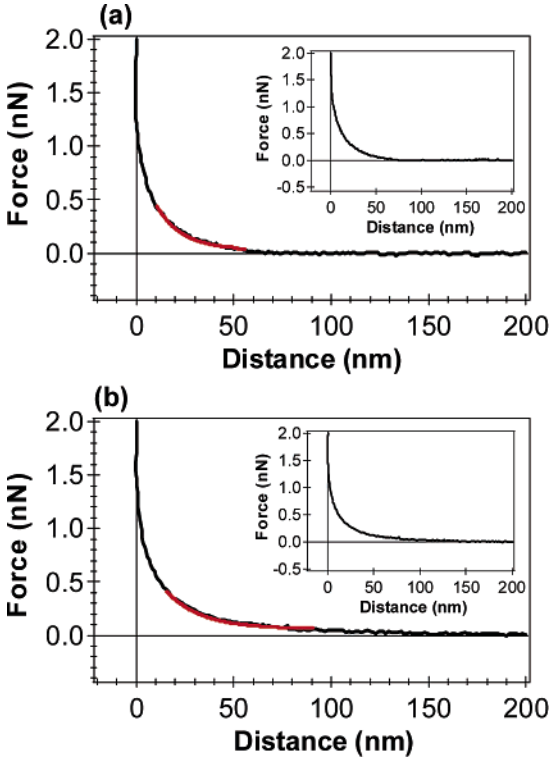

Figure 1. Approach profile of a force curve obtained in DMF between a film of poly-*N*-succinimidyl acrylate on a silicon substrate, electrografted from a 0.1 M (a) and 1 M (b) monomer solution, and a Si_3N_4 AFM tip. The red line is a fit of the compression profile by a function based on the Alexander−de Gennes model in the distance range for which the model is valid. Insets: corresponding retraction curves showing that the profile is reversible.

PNSA) between a bare silicon nitride tip and a PNSA layer on silicon grafted from a 0.1 M solution of the monomer. The monotonically increasing repulsive forces observed during the approach are the typical signature of a polymer brush under compression in a good solvent.[17] They are caused by the reduced configurational entropy of the polymer chains, which increases osmotic pressure upon approach of the surface.[18] This is a first indication that the polymer film behaves like a brush. The force profile can be represented by a function based on the Alexander−de Gennes scaling concept,[19] describing the forces resulting from the compression of polymer brushes. The Alexander−de Gennes model provides a good approximation for the calculation of the steric repulsion for moderate grafting densities (typically between 0.1 and 5 chains/100 nm^2)[17,20] but fail to describe the behavior of mushrooms and very dense brushes (above 5 chains/100 nm^2).[21] The force per unit area between an AFM tip and a surface coated with a polymer brush can be approximated by the following exponential expression, for $0.2 < D/L_0 < 0.9$:[18,20]

$$F(D) \approx 50 k_B T R L_0 \Gamma^{3/2} e^{-2\pi D/L_0} \quad (1)$$

where D is the distance between the two surfaces, R is the tip radius, L_0 is the thickness of the polymer brush, and Γ is the grafting density. From this function, the grafting density can be estimated, as illustrated in refs 17, 20, and 22 and references therein. To test whether the measured forces decay as predicted, the force profile was fitted by an exponentially decaying function:

$$F(D) = A e^{-D/z} \quad (2)$$

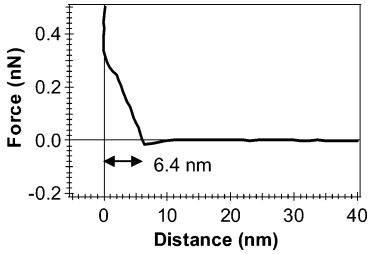

Figure 2. Approach profile of a force curve obtained in acetonitrile between a film of poly-*N*-succinimidyl acrylate on a silicon substrate, electrografted from a 0.1 M monomer solution, and a Si_3N_4 AFM tip.

where the amplitude A and the decay length z are the fitting parameters (Figure 1a, red curve). A grafting density of 0.95 ± 0.2 chains per 100 nm^2 has been estimated from this equation (average value obtained from 20 profiles recorded at different positions on the sample). That corresponds to a typical distance between grafting sites of 10.3 nm. The brush thickness is estimated at 80 nm from the decay length (using eqs 1 and 2), which is in good agreement with the onset of the repulsive forces detected in the approach profile (65 ± 10 nm). Indeed, the repulsive forces can be detected when the tip deflection deviates significantly from the baseline, i.e., when the force reaches a value of about 0.020 nN. The first steps of the compression are not detectable.

Figure 1b shows the compression profile obtained in the same conditions from a layer grafted from a 1 M monomer concentration. A grafting density of 1.1 ± 0.2 chains per 100 nm^2 has been estimated from the fitted profiles, which corresponds to a typical distance between grafting sites of 9.5 nm. There is thus no significant increase of the grafting density when increasing the monomer concentration from 0.1 to 1 M. The brush thickness is estimated at 128 nm from the decay length, which seems in good agreement with the onset of the repulsive forces detected on the approach profile (105 ± 12 nm).

Only one exponential was required to fit the approach profile, indicating that the chains are laterally immobile ("solid brush"). "Liquid brushes" (brushes with a very low grafting density or in the mushroom regime), in which chains can easily move laterally, often show more than one decaying components, characteristic of an escape transition occurring in the brush.[20,23,24] The complete reversibility of the profile (Figure 1, inset) is also a characteristic of terminally attached brushes. Adsorbed polymers often display an hysteresis between compression and decompression due to nonequilibrium relaxation effects.[17]

Force curves were also recorded in acetonitrile, a bad solvent for PNSA. The thickness of the collapsed film can be estimated from the approach profile (Figure 2). The first slope in the contact region corresponds to indentation into the polymer layer, the slope being related to the elastic modulus of the system. Then the slope change corresponds to the transition between the polymer and the silicon substrate. The thickness of the film in its collapsed state can be estimated from the extension of the first slope, i.e., 6.4 nm for a 0.1 M monomer concentration and 9.6 nm for a 1 M concentration. These values are in good agreement with the thickness measured in the dry state by ellipsometry (5.1 and 8.3 nm for a concentration of 0.1 and 1 M, respectively).

Chain Length. Recently, it was demonstrated that the stretching of individual chains away from the grafted surface with an AFM tip is a reliable approach for estimating the molecular weight of grafted polymers.[25−27] The authors validated this approach by comparison with GPC data obtained on the polymer cleaved from the surface.[26] Upon compressing the AFM

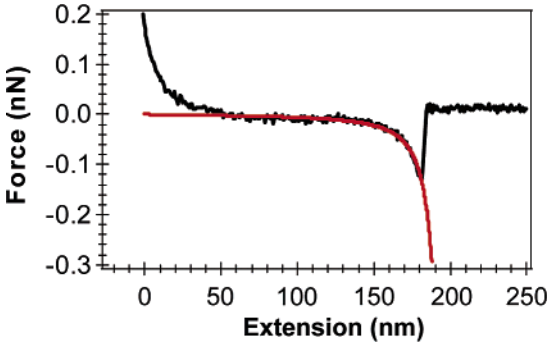

Figure 3. Force−extension curve showing a bridging interaction obtained in DMF between a film of poly-*N*-succinimidyl acrylate on a silicon substrate and a gold-coated AFM tip. The red line is a fit according to the wormlike chain model.

tip against the surface, the tip can form contacts anywhere along the chains (at a moderately high grafting density, the chain ends are located throughout the brush and not necessarily at the outer edge of the brush as this is the case at an extremely high grafting density), but it has been shown that the most probable detachment point when retracting the tip is situated at the chain end.[25−27] The detailed mechanism at the origin of the distribution of the rupture lengths is still a matter of ongoing research. Briefly, it has been proposed that upon mechanical pulling a stress is created on the chain. This stress is at first released by sliding of the polymer chain along the tip. At some point of tip/surface separation near the chain end, no more stress can be released by such sliding and significant stretching of the chain occurs, giving rise to a restoring force acting on the cantilever.[27]

We investigated the bridging interaction of the PNSA chains with the AFM tip. To force the polymer to bridge the tip, we used a gold-coated tip, the affinity of the polymer for gold being relatively high (when using a bare silicon nitride tip, bridging interaction is seldom observed). A typical retraction profile is shown in Figure 3. The rupture separation corresponds to the length of the stretched chain segment located between the grafting point on the substrate and the point of attachment to the tip. The interaction forces lie in a range of 100−400 pN, with a most probable force centered on 100 pN. The histograms of the rupture lengths are shown in Figure 4. The most probable length is centered on 155 nm (0.1 M) and 254 nm (1 M). The length of a monomer unit being 0.25 nm, we can estimate the degree of polymerization at about 620 and 1016, respectively. The rupture lengths should be corrected by an extension ratio to obtain the contour length of the chains. This ratio estimates the extent to which the chain is stretched before detaching from the tip. The extension ratio is typically determined by fitting the retraction profiles to a statistical mechanical ideal chain model, such as the wormlike chain (WLC) (or freely jointed chain, FJC) models.[28,29] The profiles have been fitted with both models (an example is shown in Figure 3). The fitting parameters are the contour length and the persistence (WLC) (or Kuhn (FJC)) length. They revealed that the chains can be stretched to about 94% of their contour length. It is worth mentioning that those statistical mechanical ideal models are strictly valid for theta conditions,[28] and we are here in good solvent conditions. The "persistence" (l_p) or "Kuhn" (l_k) lengths obtained from the fits are apparent lengths, which can deviate significantly from the true Kuhn or persistence length of a free chain in a Θ solvent. As demonstrated previously, the fits reproduce well the data for low and high force regimes, but to accurately reproduce the whole force profile, two fits are needed.[16,30] The best fit curve in the range of $F < \sim 100$ pN

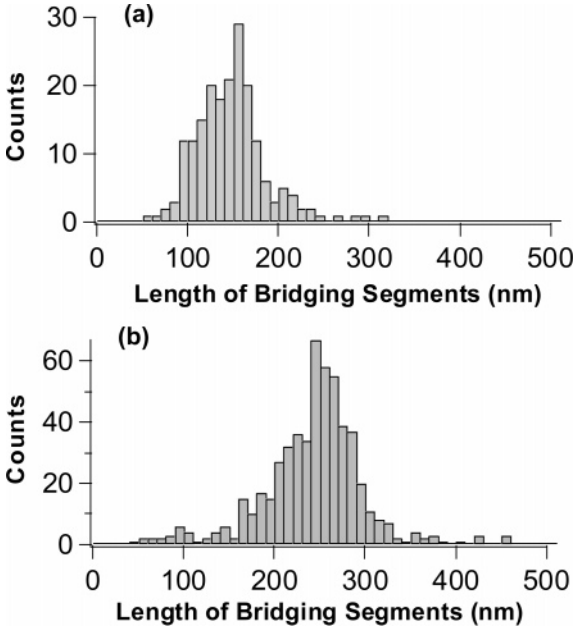

Figure 4. Distribution of the rupture separations obtained from the bridging interactions in DMF between a poly-*N*-succinimidyl acrylate film on silicon, electrografted from a 0.1 M (a) and 1 M (b) monomer solution, and a gold-coated AFM tip.

gave a $l_p = 0.95$ nm, whereas the best fit for $F > \sim 150$ pN gave a $l_p = 0.35$ nm. Above 100 pN enthalpic contributions become significant and backbone deformations prevail such that the description of the stretching by a WLC or FJC may no longer be a good approximation, and a segment elasticity must be introduced.[31] The l_p (0.35 nm) is indeed too small considering the size of the side groups. In that regime, the profile is dominated by C−C−C bond angle deformation, and the characteristic length is thus expected to be closer to the size of a monomer unit. The value of 0.95 nm seems much more reasonable; it is close to the value for polystyrene (~1 nm),[20] which has a similar backbone and bulky side groups. It is beyond the scope of this paper to discuss in detail the force curve fitting, which will be the subject of a subsequent report. The important information obtained from the fits is that the extension ratio is high; thus, we can approximate that the rupture length is equal to the contour length, considering the uncertainty on the rupture lengths (accuracy limited by the resolution with which the spring constant of the cantilever is known, among others). Thus, the correction of rupture length by the extension ratio is not critical for an estimation of the degree of polymerization.[26] It is important to note that the force profiles could be properly fitted with the models using the same apparent persistence length, which means that single molecules are indeed probed (it is a classical criterion for single molecule detection[16]), and which means also that we can exclude excessive branching in the polymers. It would have been impossible to fit the force profiles of a branched structure with realistic characteristic lengths. Fitting forces curves corresponding to highly branched polymers or multiple chains in parallel requires very low, unphysical, persistence lengths, even much lower than the size of a monomer.[32,33]

It is worth mentioning that the polydispersity is fingerprinted in the distribution of the rupture lengths. Previous studies have shown that single molecule force spectroscopy could be successfully used to evaluate the polydispersity of polymers grafted from surfaces, but the success is strongly dependent on the nature and intensity of the interaction force between the polymer and the tip (a weak interaction increases the efficiency

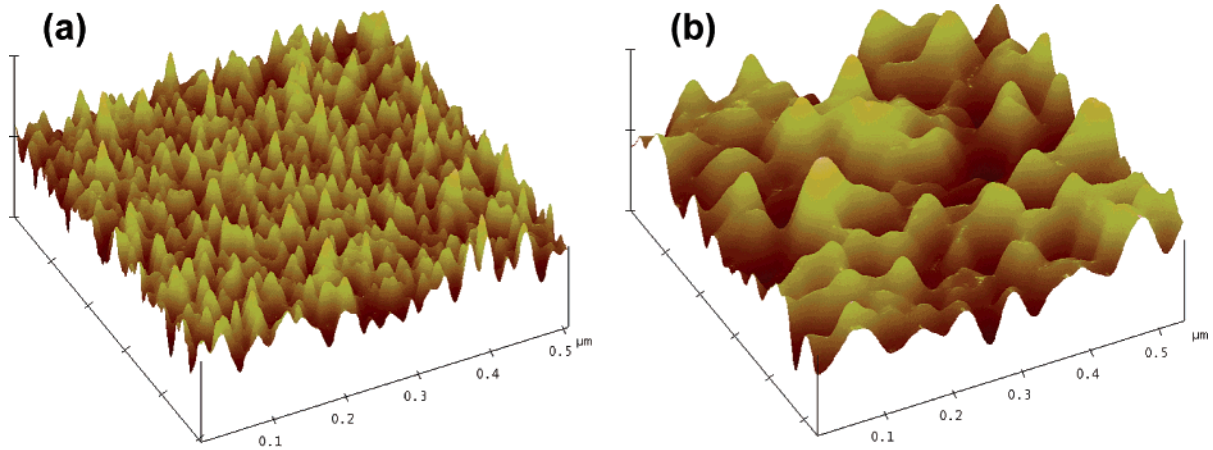

Figure 5. AFM topography images of poly-*N*-succinimidyl acrylate films on a silicon substrate grafted from a 0.1 M (a) and 1 M monomer concentration (b) (tapping mode in air, maximum *z* scale: 2 nm).

of the mechanism of sliding and thus the probability that the detachment point is indeed situated near the chain ends) and the grafting density. Since we are below the limit of grafting density above which the method could be reliably applied to provide an accurate value of the polydispersity,[26,27] it would be hazardous to estimate the polydispersity from the histogram of rupture lengths.

The scaling theory, based on the Alexander−de Gennes model, predicts that the equilibrium thickness of a polymer brush in a good solvent (L_0) varies linearly with the degree of polymerization (N), according to[18]

$$L_0 \approx Nl\left(\frac{l}{d}\right)^{2/3} \tag{3}$$

where l is the size of the statistical segments and d is the average distance between the grafting points. The statistical segment length of PNSA is not known and cannot be found in the literature, but it can be estimated at 0.67 nm, which is the value for polystyrene,[34] considering the similar backbone and bulky side groups. The statistical segment length can also be calculated from the Kuhn length ($l = (l_k l_{monomer})^{0.5}$ where $l_{monomer}$ is the length of a monomer, i.e., 0.25 nm). That gives $l = 0.69$ nm. For a degree of polymerization of 620 and a distance of 10.3 nm between grafting points, the predicted equilibrium thickness of the brush obtained from a 0.1 M monomer concentration is 72 nm, in good agreement with the value found from the fit of the compression profile (80 nm). It validates our interpretation that the most probable rupture length in the histogram corresponds indeed to the chain ends. With a degree of polymerization of 1016 for the 1 M monomer concentration and a distance of 9.5 nm between grafting sites, the predicted thickness of the swollen brush is 125 nm, also in good agreement with the value obtained from the decay length of the fit of the compression profile (128 nm).

The size of the coil (R_F) in good solvent conditions can be calculated from the degree of polymerization:[19]

$$R_F \approx lN^{3/5} \tag{4}$$

which gives a R_F of 33 nm (0.1 M) and 45 nm (1 M), about 3 and 4 times the distance between the grafting points. The chains are thus significantly stretched out from this equilibrium conformation, the layer thickness being about 3 times the size of the coil. We are thus in a moderate grafting density regime.

Figure 5 shows the topography images of the PNSA layers in the dry state. This image shows the characteristic features of

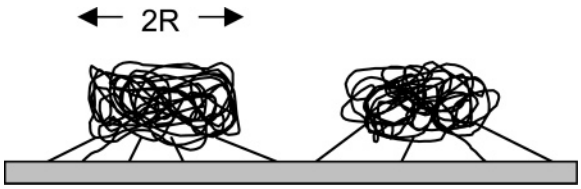

Figure 6. Schematic representation of pinned micelles.

a brush: the substrate is completely covered, the globules are close to each other, and their size is higher than the characteristic size of isolated chains. For isolated polymer chains irreversibly grafted on a surface, the theory predicts that in bad solvent conditions the chains collapse and form single globules of radius $R \approx N^{1/3}$.[35,36] For $N = 620$, it corresponds to a radius of 8.5 nm, and for $N = 1016$ to a radius of 10 nm. The diameter of the globules is thus twice higher than the distance between grafting points. A mushroom regime would require a minimum distance between grafting points of 20 nm. In this case, the theory predicts that the chains will be unable to collapse as isolated globules and they will fuse to form "pinned micelles" (see the schematic representation in Figure 6) each containing n chains,[35] and previous experimental data[36] have been shown to be consistent with this picture. The radius R of the core of a pinned micelle can be estimated from[35,36]

$$R \approx N^{3/5}\Gamma^{1/5}$$

That gives a radius of 19 and 26 nm for a monomer concentration of 0.1 and 1 M, respectively. The topography images (Figure 5) show islands 15−30 nm (0.1 M) and 40−70 nm (1 M) in diameter. Only the top part of the structures is imaged since the substrate appears completely covered. Deep valleys between the islands are inaccessible, and the tip does not probe the silicon substrate. Consequently their height is strongly underestimated.[36] Since we used sharp conical tips and since only the top part of the structures is probed, tip convolution effects on their diameter are relatively small. By using simple models of tip convolution,[36] the broadening is estimated at a few nanometers only. The diameters observed for the layer obtained from a 0.1 M monomer concentration are slightly lower than those predicted for pinned micelles and slightly higher than those predicted for isolated chains. We are thus probably at the onset of the brush regime. The values observed for the layer obtained from a 1 M monomer concentration are in good agreement with the predicted values for pinned micelles. It is worth mentioning here that the theoretical predictions hold for

bad solvent conditions with no preferential interactions with the substrate. If there is an attractive polymer−surface interaction, the globules wet the substrate, which results in a spread micelle and can account for the low aspect ratio measured.[36] The thickness measured in the dry state by ellipsometry (5.1 nm for 0.1 M and 8.3 nm for 1 M) is in agreement with a spread micelle structure, collapsed in the *z* direction.

Conclusion

The very first characterization of the structural properties of an acrylate-based polymer obtained by electrografting has been achieved by AFM force spectroscopy. Compression profiles, single molecule bridging interaction, and topography images provide an overall picture of the film structure. The results show that the electroinitiated polymerization of NSA from a silicon substrate generates a polymer brush with a grafting density of about 1 chain per 100 nm^2 and a degree of polymerization of about 620 and 1016 for a monomer concentration of 0.1 and 1 M, respectively. The structure of the electrografted film in good solvent conditions is consistent with the scaling laws predicted for a moderately dense brush system, the chains stretching out at a distance of $3R_F$ in a good solvent. The good agreement between the shape of the approach profiles and the function based on the Alexander−de Gennes scaling concept describing the forces resulting from the compression of polymer brushes, as well as the adequacy between the bridging profiles and models describing a wormlike chain and freely jointed chain under tension, are strong indications that the polymer is essentially linear with few branching points. The thickness of the swollen film in a good solvent was found to be 10 times higher than the thickness of the collapsed film in bad solvent conditions, in good agreement with ellipsometry data in the dry state. A comparison with data obtained by GPC (molecular weight and polydispersity) would help to obtain a more complete and accurate picture of the brush, but classical techniques are not easily implemented on these polymers obtained by a "grafting from" approach. Overall, this report is the very first evidence that polymers obtained by cathodic electrografting are in fact brush systems and consequently the first evidence that a polymer brush can be obtained from a direct "grafting from" method, without any intermediate layer.

Experimental Section

Materials. The *N*-succinimidyl acrylate monomer was prepared according to the procedure described in ref 37. *N*,*N*-Dimethylformamide (Aldrich, p.a.) was dried over P_2O_5 and distilled under reduced pressure. Tetraethylammonium perchlorate (TEAP) (Fluka, >99%) was heated in a vacuum at 80 °C for 12 h prior to use.

Electrografting Experiments. The electroinitiated polymerization was carried out in a one-compartment cell equipped with a Pt counter electrode and a Pt pseudo-reference—the working electrode being the silicon substrate—placed in a glovebox under a dry inert atmosphere. The monomer was dissolved in dried DMF containing tetraethylammonium perchlorate (5×10^{-2} M) as conducting salt. The electrochemical measurements were performed using an EG&G potentiostat/galvanostat (M273). All the details of the electrografting procedure and the macroscopic characterization (XPS, electrochemistry) of the resulted films are given in ref 13. The activated esters are sensitive to hydrolysis, and the samples must be kept in a dry atmosphere if they not used immediately.

AFM Experiments. Force spectroscopy experiments were carried out with a PicoSPM equipped with a fluid cell (Molecular Imaging) and controlled by Nanoscope III electronics (Digital Instruments). Silicon nitride cantilevers with a nominal spring constant of 0.05 N m^{-1} were used. Gold-coated tips were prepared following the procedure described elsewhere.[38] Prior to their use, they were cleaned by UV ozone. They were rinsed several times with ethanol and dried in a stream of nitrogen. The spring constants were calibrated using the method described in ref 39. The data were processed using a program developed in Igor Pro (WaveMetrics, Inc.) to extract from every curve the pull-off force. Topography images were recorded in tapping mode with sharp silicon tips using a Nanoscope IV scanning force microscope (Veeco).

Ellipsometry. Ellipsometry was carried out with an Elisel ellipsometer (Jobin-Yvon/Sofie instrument) operating at a wavelength of 632.8 nm. The film thickness was measured at 70.67° (incidence angle with respect to the normal of the substrate). At least five measurements were taken for each sample at different locations. The error in the thickness is about 10%. The refractive index for PNSA was 1.5.

Acknowledgment. The authors are grateful to B. Nysten (UCL) for the development of the Igor routine used for processing the force curves. They thank the Belgian Science Policy for general support in the framework of IUAP 5/03. C.J. and C.-A. Fustin are Chercheur Qualifié and Chargé de Recherches of the Belgian National Fund for Scientific Research (FNRS), respectively.

References and Notes

(1) Maboudian, R. *Surf. Sci. Rep.* **1998**, *30*, 209−270.
(2) Yates, J. T. *Science* **1998**, *279*, 335−336.
(3) LeMieux, M. C.; Julthongpiput, D.; Bergman, K. N.; Cuong, P. D.; Ahn, H. S.; Lin, Y. H.; Tsukruk, V. V. *Langmuir* **2004**, *20*, 10046−10054.
(4) Bumbu, G.-G.; Kircher, G.; Wolkenhauer, M.; Berger, R.; Gutmann, J. S. *Macromol. Chem. Phys.* **2004**, *205*, 1713−1720.
(5) Prucker, O.; Rühe, J. *Macromolecules* **1998**, *31*, 592−601.
(6) (a) Zhao, B.; Brittain, W. J. *Prog. Polym. Sci.* **2000**, *25*, 677−710. (b) Boyes, S. G.; Granville, A. M.; Baum, M.; Akgun, B.; Mirous, B. K.; Brittain, W. J. *Surf. Sci.* **2004**, *570*, 1−12.
(7) Matyjaszewski, K.; Xia, J. *Chem. Rev.* **2001**, *101*, 2921−2990.
(8) Edmondson, S.; Osborne, V. L.; Huck, W. T. S. *Chem. Soc. Rev.* **2004**, *33*, 14−22.
(9) For a review on electro-initiated polymerization see: (a) Baute, N.; Jérôme, C.; Martinot, L.; Mertens, M.; Geskin, V. M.; Lazzaroni, R.; Brédas, J. L.; Jérôme, R. *Eur. J. Inorg. Chem.* **2001**, 1097−1107. (b) Palacin, S.; Bureau, C.; Charlier, J.; Deniau, G.; Mouanda, B.; Viel, P. *ChemPhysChem* **2004**, *5*, 1468−1481. (c) Jérôme, C.; Jérôme, R. In *Stimuli-Responsive Polymeric Films and Coatings;* Urban, M., Ed.; ACS symposium Series 912; American Chemical Society: Washington, DC,2005; Chapter 6, pp 85−104.
(10) Detrembleur, C.; Jérôme, C.; Claes, M.; Louette, P.; Jérôme, R. *Angew. Chem., Int. Ed.* **2001**, *40*, 1268−1271.
(11) Ignatova, M.; Voccia, S.; Gilbert, B.; Markova, N.; Mercuri, P. S.; Galleni, M.; Sciannamea, V.; Lenoir, S.; Cossement, D.; Gouttebaron, R.; Jérôme, R.; Jérôme, C. *Langmuir* **2004**, *20*, 10718−10726.
(12) Ameur, S.; Bureau, C.; Charlier, J.; Palacin, S. *J. Phys. Chem. B* **2004**, *108*, 13042−13046.
(13) Jérôme, C.; Gabriel, S.; Voccia, S.; Detrembleur, C.; Ignatova, M.; Gouttebaron, R.; Jérôme, R. *Chem. Commun.* **2003**, 2500−2501.
(14) Jérôme, C.; Aqil, A.; Voccia, S.; Labaye, D. E.; Maquet, V.; Gautier, S.; Bertrand, O. F.; Jérôme, R. *J. Biomed. Mater. Res.* **2006**, *76A*, 521−529.
(15) Gabriel, S.; Dubruel, P.; Schacht, E.; Jonas, A. M.; Gilbert, B.; Jérôme, R.; Jérôme, C. *Angew. Chem., Int. Ed.* **2005**, *44*, 2−6.
(16) For a review on single molecule force Spectroscopy on synthetic polymers see: Hugel, T.; Seitz, M. *Macromol. Rapid Commun.* **2001**, *22*, 989−1016.
(17) Taunton, H. J.; Toprakcioglu, C.; Fetters, L. J.; Klein, J. *Nature (London)* **1988**, *332*, 712−714.
(18) Israelachvili, J. *Intermolecular and Surface Forces*; Academic Press: San Diego, 1991.
(19) de Gennes, P. G. *Adv. Colloid Interface Sci.* **1987**, *27*, 189−209.
(20) Butt, H.-J.; Kappl, M.; Mueller, H.; Raiteri, R.; Meyer, W.; Rühe, J. *Langmuir* **1999**, *15*, 2559−2565.
(21) Yamamoto, S.; Ejaz, M.; Tsujii, Y.; Fukuda, T. *Macromolecules* **2000**, *33*, 5608−5612.
(22) Duwez, A. S.; Guillet, P.; Colard, C.; Gohy, J. F.; Fustin, C. A. *Macromolecules* **2006**, *39*, 2729−2731.
(23) Guffond, M. C.; Williams, D. R. M.; Sevick, E. M. *Langmuir* **1997**, *13*, 5691−5696.
(24) Jimenez, J.; Rajagopalan, R. *Langmuir* **1998**, *14*, 2598−2601.

(25) Goodman, D.; Kizhakkedathu, J. N.; Brooks, D. E. *Langmuir* **2004**, *20*, 3297−3303.
(26) Goodman, D.; Kizhakkedathu, J. N.; Brooks, D. E. *Langmuir* **2004**, *20*, 6238−6245.
(27) Al-Maawali, S.; Bemis, J. E.; Akhremitchev, B. B.; Leecharoen, R.; Janesko, B. G.; Walker, G. C. *J. Phys. Chem. B* **2001**, *105*, 3965−3971.
(28) Flory, P. J. *Statistical Mechanics of Chain Molecules;* Hanser: Muenchen, 1989.
(29) (a) Fixman, M.; Kovac, J. *J. Chem. Phys.* **1973**, *58*, 1564−1568. (b) Smith, S. B.; Finzi, L.; Bustamante, C. *Science* **1992**, *258*, 1122−1126. (c) Bustamante, C.; Marko, J. F.; Siggia, E. D. *Science* **1994**, *265*, 1599−1600. (d) Marko, J. F.; Siggia, E. D. *Macromolecules* **1995**, *28*, 8759−8770.
(30) Hugel, T.; Grosholz, M.; Clausen-Schaumann, H.; Pfau, A.; Gaub, H. E.; Seitz, M. *Macromolecules* **2001**, *34*, 1039−1047.
(31) Odijk, T. *Macromolecules* **1995**, *28*, 7016−7018.
(32) Bemis, J. E.; Akhremitchev, B. B.; Walker, G. C *Langmuir* **1999**, *15*, 2799−2805.
(33) Thompson, J. B.; Kindt, J. H.; Drake, B.; Hansma, H. G.; Morse, D. E.; Hansma, P. K. *Nature (London)* **2001**, *414*, 773−776.
(34) Karim, A.; Satija, S. K.; Douglas, J. F.; Ankner, J. F.; Fetters, L. J. *Phys. Rev. Lett.* **1994**, *73*, 3407−3410.
(35) Zhulina, E. B.; Birshtein, T. M.; Priamitsyn, V. A.; Klushin, L. I. *Macromolecules* **1995**, *28*, 8612−8620.
(36) Koutsos, V.; vanderVegte, E. W.; Pelletier, E.; Stamouli, A.; Hadzioannou, G. *Macromolecules* **1997**, *30*, 4719−4726.
(37) Batz, H.-G.; Franzmann, G.; Ringsdorf, H. *Angew. Chem., Int. Ed.* **1972**, *11*, 1103−1104.
(38) Duwez, A.-S.; Poleunis, C.; Bertrand, P.; Nysten, B. *Langmuir* **2001**, *17*, 6351−6357.
(39) Dupres, V.; Menozzi, F. D.; Locht, C.; Clare, B. H.; Abbott, N. L.; Cuenot, S.; Bompard, C.; Raze, D.; Dufrêne, Y. F. *Nat. Methods* **2005**, *2*, 515−520.

MA060824M